

# GLP-1(9-36), a GLP-1 cleavage product, protects against oxidative stress and apoptosis through PI3K/Akt/NOS pathway in H9c2 cardiomyoblasts

Narawat Nuamnaichati

Mahidol University

Warisara Parichatikanond

Mahidol University

Supachoke Mangmool (✉ [supachoke.man@mahidol.ac.th](mailto:supachoke.man@mahidol.ac.th))

Mahidol University

---

## Research Article

**Keywords:** Akt, Apoptosis, GLP-1(9-36), GLP-1R, NOS, Oxidative stress, PI3K

**Posted Date:** June 9th, 2021

**DOI:** <https://doi.org/10.21203/rs.3.rs-593914/v1>

**License:**  This work is licensed under a Creative Commons Attribution 4.0 International License.

[Read Full License](#)

---

## Abstract

GLP-1(7–36), a major active form of GLP-1 hormone, is rapidly cleaved by dipeptidyl peptidase-4 to generate a truncated metabolite, GLP-1(9–36) which has a low affinity for GLP-1 receptor (GLP-1R). GLP-1(7–36) has been shown to have protective effects on cardiovascular system through GLP-1R-dependent way. Nevertheless, the cardioprotective effects of GLP-1(9–36) have not fully understood. The present study investigated the effects of GLP-1(9–36), including its underlying mechanisms against oxidative stress and apoptosis in H9c2 cardiomyoblasts. Here, we reported that GLP-1(9–36) protects H9c2 cardiomyoblasts from hydrogen peroxide ( $H_2O_2$ )-induced oxidative stress by promoting the synthesis of antioxidant enzymes, glutathione peroxidase-1, catalase, and heme oxygenase-1. In addition, treatment with GLP-1(9–36) suppressed  $H_2O_2$ -induced apoptosis by attenuating caspase-3 activity and upregulating proapoptotic proteins, Bcl-2 and Bcl-xL. These protective effects of GLP-1(9–36) are attenuated by blockade of PI3K-mediated Akt phosphorylation and prevention of nitric oxide synthase (NOS)-induced NO production. Collectively, GLP-1(9–36) represents the potential therapeutic target for prevention of oxidative stress and apoptosis in the heart.

## Introduction

Cardiovascular complications constitute the major cause of morbidity and mortality in type II diabetes mellitus (DM) patients<sup>1,2</sup>. Patients with type II DM have high incidence of death from heart diseases compared to non-diabetic persons<sup>3,4</sup>. Numerous cardiovascular abnormalities and diseases, including hypertension, heart failure (HF), myocardial ischemia and infarction are associated with oxidative stress<sup>5,6</sup>. Oxidative stress is an imbalance between production of reactive oxygen species (ROS) and antioxidant defense mechanisms. Excessive ROS production leads to apoptosis and death of cardiac myocytes, which have been implicated in the loss of cardiac functions, leading to development of HF<sup>7</sup>. Although the pathophysiology of HF is complicated, oxidative stress seems to be an essential therapeutic target for improving the cardiac performances. Thus, prevention of oxidative stress and apoptosis during cardiac injury might improve and slow disease progression of HF.

Glucagon-like peptide-1 (GLP-1) is an incretin peptide hormone secreted from the intestinal L cells in the response to food intake. Two active forms of GLP-1 are GLP-1(7-36) and GLP-1(7-37). The majority of circulating active GLP-1 is in the form of GLP-1(7-36), which binds to and stimulates GLP-1 receptor<sup>8,9</sup>. GLP-1Rs are widely expressed in many tissues, including the heart, and previous studies indicated that GLP-1 and its analogues (GLP-1R agonists) exert cytoprotective effects and play an essential role in modulation of heart functions. For instance, treatment with exendin-4 (GLP-1R agonist) provokes antioxidant and antiapoptotic effects through GLP-1 receptor-dependent manner in cardiac myocytes<sup>10</sup>. Administration of GLP-1(7-36) enhanced cell survival and restored myocardial functions after ischemia-reperfusion injury<sup>11</sup>. In addition, activation of GLP-1R attenuated methylglyoxal (MG)-induced mitochondrial dysfunctions in H9c2 cardiomyoblasts<sup>12</sup>.

GLP-1(7-36) has a very short half-life (about 2 minutes) and is rapidly cleaved by dipeptidyl peptidase-4 (DPP-4) at its N-terminus to generate GLP-1(9-36)<sup>9</sup>. Since GLP-1(9-36) has weak interaction with GLP-1R and has no significant effects on stimulation of insulin secretion or glucose homeostasis, it was previously assumed as an inactive GLP-1 metabolite<sup>13,14</sup>. Interestingly, administration of GLP-1(9-36) reduced the mitochondrial ROS levels in the hippocampus of amyloid precursor protein/presenilin1 (APP/PS1) mice<sup>15</sup>. Continuous infusion of GLP-1(9-36) increased myocardial glucose uptake and improved left ventricular performance and systemic hemodynamics in dog model with dilated cardiomyopathy<sup>16</sup>. GLP-1(9-36) was observed to exert antioxidant effects on cultured cardiac cells of Goto-Kakizaki rats<sup>17</sup>. The protective effects of GLP-1(9-36) were found in the conditions of GLP-1R blockade. Administration of GLP-1(9-36) increased coronary blood flow and possessed vasodilatory effects of mesenteric arteries in both wild-type and GLP-1R knockout mice<sup>11</sup>. Moreover, the effects of GLP-1(9-36) were attenuated in a presence of GLP-1R antagonist, exendin(9-39)<sup>18</sup>. Thus, GLP-1(9-36), an active metabolite of GLP-1, exhibits protective effects through GLP-1R-independent pathway. Nevertheless, the signal transduction of GLP-1(9-36) for antioxidant and antiapoptotic effects in the heart has not fully understood.

The PI3K/Akt signaling pathway implicated various cell functions, including cell survival, proliferation and differentiation<sup>19</sup>. When oxidative stress occurs, this PI3K/Akt signaling pathway is activated and further inhibition of apoptosis<sup>20</sup>. Upregulation of PI3K signaling was able to protect cardiac myocytes from apoptosis and cell death in ischemia and reperfusion (I/R)-induced oxidative damage<sup>21</sup>. PI3K and Akt modulated their downstream effectors, including nitric oxide synthase (NOS) by phosphorylation. Treatment with GLP-1(9-36) induced vasodilation and upregulation of eNOS, indicating that NO is necessary for GLP-1(9-36)-mediated vasodilatory effects in human umbilical vein endothelial cells (HUVECs)<sup>22</sup>. In human endothelial cells, GLP-1(9-36) improved cell survival undergoing I/R injury via NO-dependent way<sup>18</sup>. Overproduction of H<sub>2</sub>O<sub>2</sub> is associated with cell injury and tissue damage in I/R model<sup>23</sup> and H<sub>2</sub>O<sub>2</sub> is widely used for induction of apoptosis<sup>24</sup>. In our present study, we used H<sub>2</sub>O<sub>2</sub> as the inducer of oxidative stress and apoptosis in H9c2 cardiomyoblasts. The protective effects of GLP-1(9-36) might be independent of GLP-1R signaling pathway. However, the underlying mechanisms and signaling pathway of GLP-1(9-36) in the heart have not completely clarified. In the present study, we aimed to evaluate the cardioprotective effects of GLP-1(9-36) against of H<sub>2</sub>O<sub>2</sub>-induced oxidative stress and apoptosis in H9c2 cardiomyoblasts.

## Results

### **GLP-1(9-36) mediates antioxidant and antiapoptotic effects via GLP-1R-independent pathway.**

We investigated the protective effects of GLP-1(9-36) and exendin-4 (DPP-4-resistant GLP-1R agonist) on H<sub>2</sub>O<sub>2</sub>-induced oxidative stress and apoptosis. Exposure of H9c2 cells to H<sub>2</sub>O<sub>2</sub> robustly increased intracellular ROS production compared to control (vehicle-treated) cells (Fig. 1A). Treatment with GLP-1(9-

36) significantly inhibited H<sub>2</sub>O<sub>2</sub>-induced intracellular ROS levels and apoptosis in a concentration-dependent manner that shown the highest effects at a concentration of 40 nM (Fig. 1A,B), indicating that GLP-1(9-36) inhibited oxidative stress and apoptosis induced by H<sub>2</sub>O<sub>2</sub>. We compared the antioxidant and antiapoptotic effects of GLP-1(9-36) versus exendin-4 (GLP-1R agonist). Treatment with either exendin-4 (GLP-1R agonist) or GLP-1(9-36) significantly decreased H<sub>2</sub>O<sub>2</sub>-induced intracellular ROS production. In contrast, preincubation with exendin-(9-39) (a selective GLP-1R antagonist) reversed this antioxidant effect of exendin-4, but not GLP-1(9-36).

We also used dihydroethidium (DHE) staining assay to confirm the cellular antioxidant effects of these peptides. The H<sub>2</sub>O<sub>2</sub>-exposed cells had a significant increase in the fluorescence signals of DHE oxidation products as shown in the red color (Fig. 1D). Treatment with GLP-1(9-36) caused a significant reduction in the red fluorescent intensities which has similar effects to those of exendin-4. Blockade of GLP-1R with exendin-(9-39) completely inhibited the antioxidant effect of exendin-4, but not GLP-1(9-36) (Fig. 1D). These results indicated that GLP-1(9-36) possesses antioxidant effects by reducing intracellular ROS production through GLP-1R-independent way.

To examine the antiapoptotic effects of exendin-4 and GLP-1(9-36), TUNEL staining and caspase-3 activity assays were performed in H9c2 cardiomyoblasts. Treatment with either exendin-4 or GLP-1(9-36) protected the cells from H<sub>2</sub>O<sub>2</sub>-induced apoptosis (Fig. 1E) and these two peptides also reduced caspase-3 activity induced by H<sub>2</sub>O<sub>2</sub> (Fig. 1F) in H9c2 cells. Whereas pretreatment with exendin-(9-39) significantly blocked antiapoptotic effects of exendin-4, but not GLP-1(9-36), suggesting that GLP-1(9-36) does not exert its antiapoptotic effects through GLP-1 receptor.

### **GLP-1(9-36) inhibits H<sub>2</sub>O<sub>2</sub>-induced oxidative stress and apoptosis in cAMP-independent manner**

Stimulation of GLP-1R leads to the elevation of cAMP levels through activation of adenylate cyclase (AC) activity. Because both GLP-1R agonists (GLP-1(7-36) and exendin-4) and GLP-1(9-36) have significant vasodilatory effects on isolated rat aorta and these effects appears to be mediated, at least partially via cAMP<sup>25</sup>, we investigated whether the protective effects of GLP-1(9-36) is mediated through cAMP-dependent pathway. Pretreatment with either 2¢, 5¢-dideoxyadenosine (DDA; AC inhibitor), PKI (PKA inhibitor), or ESI-09 (Epac inhibitor) did not block antioxidant effects (Fig. 2A,B) and antiapoptotic effects of GLP-1(9-36) (Fig. 2C,D). Stimulation of GLP-1Rs with exendin-4 robustly increased the cAMP levels while pretreatment with DDA completely inhibited exendin-4-mediated cAMP production (Fig. 2E). However, treatment with GLP-1(9-36) tended to increase cAMP levels, to a lesser extent than exendin-4 (Fig. 2E). Therefore, these results imply that cAMP and its effectors (PKA and Epac) do not involved in GLP-1(9-36)-mediated antioxidant and antiapoptosis in H9c2 cardiomyoblasts.

### **PI3K/Akt/NOS axis is required for antioxidant and antiapoptotic effects of GLP-1(9-36)**

It has been shown that activation of PI3K and Akt contributes to inhibition of oxidative stress and apoptosis<sup>20,26</sup>. To determine whether the PI3K, Akt and NOS are involved in the cardioprotective effects of

GLP-1(9-36), various specific inhibitors for PI3K, Akt and NOS were used in this study. As shown in Fig. 3, pretreatment with LY294002 (PI3K inhibitor), Akti-1/2 (Akt inhibitor), and L-NAME (NOS inhibitor) but not PKC(19-36) (PKC inhibitor) significantly inhibited GLP-1(9-36)-mediated inhibition of ROS production induced by H<sub>2</sub>O<sub>2</sub> (Fig. 3A, B). In addition, LY294002, Akti-1/2, and L-NAME also reversed the antiapoptotic effects of GLP-1(9-36) in H9c2 cardiomyoblasts (Fig. 3C,D). Therefore, these results indicated that PI3K, Akt, and NOS are necessary for the cardioprotective effects of GLP-1(9-36) against oxidative stress and apoptosis.

Akt is one of the major downstream targets of PI3K. As Akt is phosphorylated and activated by PI3K, we next confirmed whether blockades of PI3K and Akt activities are capable for suppressing GLP-1(9-36)-mediated phosphorylation of Akt. After treatment with either exendin-4 or GLP-1(9-36), the phosphorylated Akt (p-Akt) levels significantly increased, whereas exendin-4-induced Akt phosphorylation was suppressed by exendin-9-39 (Fig. 4A). In contrast, blockade of GLP-1R with exendin-9-39 had no effect on GLP-1(9-36)-mediated Akt phosphorylation (Fig. 4A). In addition, GLP-1(9-36)-mediated Akt phosphorylation was significantly reduced by either LY294002 (PI3K inhibitor) or Akti-1/2 (Akt inhibitor) (Fig. 4B). Taken together, stimulation of Akt activity can occur through 1) GLP-1R-dependent pathway by exendin-4 and 2) GLP-1R-independent manners by GLP-1(9-36).

As Akt can activate NOS, resulting in an increase of NO production, we further determined the effects of GLP-1(9-36) on NO production in H9c2 cells. As shown in Fig. 4C, treatment with GLP-1(9-36) induced NO production. Additionally, treatment with lipopolysaccharide (LPS; potent inducer of inflammation) robustly increased NO production via eNOS activity. Although the high levels of NO induced by LPS leads to cell injury, however the amount of NO induced by GLP-1(9-36) was lower than LPS (Fig. 4C). Moreover, GLP-1(9-36)-mediated NO production was significantly inhibited by either LY294002, Akti-1/2 or L-NAME (NOS inhibitor) (Fig. 4D). In addition, treatment with GLP-1(9-36) significantly increased the mRNA expressions of nNOS and eNOS in H9c2 cells (Fig. 4E), indicating that GLP-1(9-36)-induced NO production is derived from the upregulation of nNOS and eNOS. These data strongly suggested that GLP-1(9-36) exhibits cardioprotective effects by regulating nitric oxide production via PI3K/Akt/NOS signaling pathway.

### **GLP-1(9-36) upregulates the synthesis of antioxidant enzymes and antiapoptotic proteins**

Antioxidant enzymes such as GPx-1, catalase, HO-1, and SODs, are one of the defensive strategies against oxidative damage in various cell types. Therefore, we analyzed an antioxidative mechanism of GLP-1(9-36) under oxidative stress by measuring the mRNA and protein expressions of these antioxidant enzymes. Treatment with GLP-1(9-36) significantly increased mRNA and protein expression levels of GPx-1, catalase, and HO-1 which are similar to those of exendin-4 treated group (Fig. 5A,D). In addition, we also evaluated the effects of GLP-1(9-36) on the upregulation of antiapoptotic and proapoptotic proteins. Exposure of H9c2 cells to GLP-1(9-36) elevated both mRNA and protein levels of antiapoptotic Bcl-2 and Bcl-xL (Fig. 5B,E). Treatment with GLP-1(9-36) also suppressed H<sub>2</sub>O<sub>2</sub>-induced mRNA expression of proapoptotic Bad and Bax (Fig. 5C). These results proposed that GLP-1(9-36) exerts the antioxidative

properties by increasing antioxidant enzyme synthesis and protects against apoptosis by inducing antiapoptotic Bcl-2 and Bcl-xL synthesis, and also reducing H<sub>2</sub>O<sub>2</sub>-mediated proapoptotic Bad and Bax expression.

### **GLP-1(9-36)-mediated the upregulation of antioxidant enzymes and antiapoptotic proteins is dependent of PI3K/Akt/NOS signaling pathway**

We investigated whether the upregulation of antioxidant and antiapoptotic markers by GLP-1(9-36) depends on activation of PI3K/Akt/NOS pathway, but not cAMP-dependent pathway. As shown in Fig. 6A, treatment with GLP-1(9-36) increased protein expression levels of catalase, GPx-1, and HO-1 even in the presence of either DDA, PKI, or ESI-09, suggesting that cAMP and its effectors, PKA and Epac, did not involve in GLP-1(9-36)-mediated this effect. Blockades of PI3K by LY294002, Akt by Akti-1/2, or NOS by L-NAME significantly reduced GLP-1(9-36)-mediated catalase, GPx-1 and HO-1 synthesis (Fig. 6B).

In addition, GLP-1(9-36) treatment led to the elevation of Bcl-2 and Bcl-xL protein levels in H9c2 cardiomyoblasts (Fig. 7). Inhibitions of AC activity by DDA, PKA activity by PKI, or Epac activity by ESI-09 had no effects on GLP-1(9-36)-mediated antiapoptotic Bcl-2 and Bcl-xL synthesis (Fig. 7A). In contrast, GLP-1(9-36)-induced the synthesis of Bcl-2 and Bcl-xL were potently reduced by blockades of PI3K, Akt, and NOS activities, but not PKC activity (Fig. 7B).

Therefore, these results confirmed that GLP-1(9-36) increases the productions of antioxidant enzymes and antiapoptotic proteins in a PI3K/Akt/NOS-dependent manner.

## **Discussion**

In the present study, we provided for the first time that a truncated metabolite of GLP-1 hormone, GLP-1(9–36) rescued oxidative stress and apoptosis in H9c2 cardiomyoblasts through PI3K/Akt/NOS signaling pathway. This protective role is likely by ways of increasing the production of antioxidant enzymes, GPx-1, catalase, HO-1, inactivation of caspase-3 apoptotic pathway, and upregulation of antiapoptotic proteins, Bcl-2, Bcl-xL.

Since oxidative stress is primarily caused by imbalance between oxidants and antioxidants, overproduction of ROS can potentially trigger the processes of DNA fragmentation, protein and lipid oxidations and is considered as one of the major contributions to apoptosis and cell death<sup>27,28</sup> (Kim and Kang, 2010). In the heart, oxidative stress and apoptosis are related to the pathological processes of ischemia and play an essential role in the progression and development of heart diseases<sup>28–30</sup>. H<sub>2</sub>O<sub>2</sub> can act as the destructive molecule that involved in most of the redox reactions in the cells, and a high level of H<sub>2</sub>O<sub>2</sub> is one of the major causes of myocardial I/R injury<sup>23</sup>. According to H<sub>2</sub>O<sub>2</sub> is widely used in models for myocardial I/R injury which leads to reduced antioxidant activity and also induced cell death<sup>24,31</sup>, in the present study, we used H<sub>2</sub>O<sub>2</sub> as a inducer of oxidative stress and apoptosis in H9c2 cells. Therefore,

the inhibition of oxidative stress and apoptosis induced by H<sub>2</sub>O<sub>2</sub> in cardiac cells may be an effective way to prevent myocardial I/R injury and improve cardiac function after cardiac injury.

GLP-1 and its analogs (GLP-1R agonists; exenatide, liraglutide) were intensively studied to find their cardioprotective effects against cardiac injury. GLP-1 is an incretin hormone which is produced in the gut in response to food intake. GLP-1 has two active isoform; GLP-1(7–36) and GLP-1(7–37)<sup>8,9</sup>. In the circulatory system, approximately 80% of total GLP-1 hormone is GLP-1(7–36), which is rapidly cleaved by enzyme DPP-4 to GLP-1(9–36)<sup>32</sup>. Due to GLP-1(9–36) has no significant effects on insulin secretion and weak interaction to GLP-1R, it was previously recognized as a truncated inactive metabolite of GLP-1(9–37)<sup>13</sup>. Over the past decade, accumulated reports have demonstrated the protective effects of GLP-1(9–36) in many tissues, including the heart. Treatment with both exendin-4 (GLP-1R agonist) and GLP-1(9–36) provoked protective effects against MG-induced mitochondrial dysfunction through GLP-1R-dependent and GLP-1R-independent manner, respectively in H9c2 cells<sup>12</sup>. In dog with dilated cardiomyopathy model, administration of GLP-1(9–36) induced myocardial glucose uptake and improved LV function<sup>16</sup>. In contrast to GLP-1(7–36), GLP-1(9–36) suppressed high glucose-induced superoxide production in human arterial endothelial cells<sup>15</sup>. In addition, GLP-1(9–36) ameliorated cell survival in response to I/R injury and hydrogen peroxide treatment in human aortic endothelial cells<sup>18</sup>. Moreover, GLP-1(9–36) suppressed mitochondrial ROS production induced by high glucose in human endothelial cells<sup>33</sup>. Consistently with these previous studies, we also observed that GLP-1(9–36) treatment strongly inhibited H<sub>2</sub>O<sub>2</sub>-induced ROS production and caspase-3 activity in H9c2 cardiomyoblasts. These data imply that GLP-1(9–36) possesses cardioprotective effects through inhibition of oxidative stress and apoptosis. Exendin-4 is a peptide isolated from the saliva of the gila monster lizard which shows about 53% amino acid sequence homology with GLP-1 hormone.

Exendin-4 is resistant to DPP-4 cleavage and acts as a potent GLP-1R agonist<sup>34</sup>. Interestingly, exendin-4 represented antioxidant and antipoptotic effects appeared to be greater than that of GLP-1(9–36) in H9c2 cardiomyoblasts against the same H<sub>2</sub>O<sub>2</sub> concentration (Fig. 1). Indeed, the molecular mechanism for these effects of GLP-1(9–36) is different from that of GLP-1R agonist. GLP-1(9–36) is further cleaved by neutral endopeptidase to generate GLP-1(28–36)<sup>35</sup>. GLP-1(28–36) prevented myocardial ischemic injury and also reduced myocardial infarct size in mice model of ischemic injury<sup>36</sup>. However, it remains an unsolved question whether GLP-1(28–36), a cleavage product of GLP-1(9–36), exhibits antioxidant and antiapoptotic effects.

The death of cardiac cells from apoptosis causes a significant loss in cardiac functions. Therefore, several studies have focused on the ways to protect cardiac myocytes from pathological stimuli, including oxidative stress. Due to its importance in the cardiac contractility, cardiac myocyte seems to have defense mechanisms itself against oxidative stress<sup>37</sup>. One of these mechanisms of cardiac myocytes could be an induction of antioxidant enzyme production, including its activity. Various types of antioxidant enzymes (e.g., catalase, GRe, GPx, SOD, HO-1) are the major components for scavenging the reactive free radicals in many cell types. These antioxidant abilities of GLP-1 are believed to arise from

enhancement of GLP-1 signaling leading to upregulation of antioxidant enzyme synthesis. For example, GLP-1 prevented ROS-mediated endothelial cell senescence by inducing the synthesis of HO-1 and NQO1 in HUVECs<sup>38</sup>. Stimulation of GLP-1R significantly inhibited oxidative stress in the liver of diabetic mice by upregulating catalase, GPx, and SOD<sup>39</sup>. These antioxidant mechanisms of GLP-1 are mediated through GLP-1 receptor-dependent manner. In the same way, antioxidant effects of GLP-1 cleavage product, GLP-1(9–36) might be due to the upregulation of antioxidant enzyme synthesis in cardiac cells. We found that GLP-1(9–36) leads to the significant upregulations of GPx-1, catalase, and HO-1 (Fig. 5). Interestingly, GLP-1(9–36)-mediated the upregulation of GPx-1, catalase, and HO-1 synthesis was not inhibited by either AC inhibitor or Epac inhibitor, indicating that the upregulation of these antioxidant enzymes by GLP-1(9–36) is independent of GLP-1R/cAMP/PKA signaling pathway in H9c2 cardiomyoblasts.

Apoptosis or death of cardiac cells is a key regulator in the pathogenesis of ischemic heart diseases especially after myocardial infarction, and the Bcl-2 family proteins are known as key regulators of apoptotic response. Bcl-2 family belongs to a group of apoptosis-regulating proteins and consists of two subgroups which are important to either inhibiting apoptosis (antiapoptotic proteins; Bcl-2, Bcl-xL, and Bcl-W) and promotes apoptosis (pro-apoptotic proteins; Bad, Bak, Bax, and Bid)<sup>40</sup>. Bcl-2 and Bcl-xL, are essential to the cell survival and have ability to prevent cardiac myocytes from detrimental outcomes in response to various stimuli. In addition, Bax and Bad expression integrates important functions that are related to apoptosis and facilitate the release of cytochrome c from mitochondria<sup>41</sup>. Caspases are a family of cysteine proteases that serve as key regulators in programmed cell death or apoptosis. Among them, caspase-3 frequently activates apoptosis for catalyzing the specific cleavage and activation of many effectors, including caspase-6, caspase-7, and SREBPs<sup>42</sup>. Thus, upregulation of Bcl-2 and Bcl-xL, downregulation of Bad and Bax, and inhibition of caspase-3 activity are regarded as the hallmarks of antiapoptotic ability. Here, we demonstrated that treatment with GLP-1(9–36) increased the expressions of Bcl-2 and Bcl-xL, whereas the expressions of Bad and Bax were not changed. In addition, GLP-1(9–36) reduced the expression of Bad and Bax induced by H<sub>2</sub>O<sub>2</sub> in H9c2 cardiomyoblasts (Fig. 5). These findings indicated that GLP-1(9–36) provokes pro-survival signaling pathways in the normal and H<sub>2</sub>O<sub>2</sub>-treated conditions, leading to improved apoptosis and enhanced cell survival after oxidative stress in the heart.

As we known that GLP-1(9–36) was considered to be an inactive peptide, thus, it might have the other signaling for GLP-1(9–36)-mediated protective effects which is independent of GLP-1 receptor. For instance, GLP-1(9–36) provoked cardioprotective effects against MG-induced mitochondrial dysfunction<sup>12</sup>. The cardioprotective and vasodilatory effects of GLP-1(7–36) are still observed even in GLP-1R knockout mice, which implied the beneficial roles of GLP-1(9–36) in GLP-1R independent fashion<sup>11</sup>. Consistent with these studies, we demonstrated that the antioxidant and antiapoptotic effects of GLP-1(9–36) were independent of GLP-1R.

After exendin-4 binding to GLP-1R, this leads to the coupling and activation of Gas protein by GLP-1R, resulting in an increase of cAMP levels through the activated AC. After that cAMP binds to and interacts with its effectors, including PKA and Epac. Elevation of cAMP levels by GLP-1R stimulation have been

shown to have cardioprotective effects in mouse cardiomyocytes<sup>43</sup> and H9c2 cardiomyoblasts<sup>12</sup>. Although treatment with GLP-1(9–36) increased cAMP levels, this effect of GLP-1(9–36) was less than that of exendin-4 (a potent GLP-1R agonist) (Fig. 2E). In addition, blockade of AC activity by DDA had no effect on GLP-1(9–36)-mediated antioxidant and antiapoptotic effects in H9c2 cardiomyoblasts, emphasizing cardioprotective effects of GLP-1(9–36) are not mediated through cAMP-signaling pathway. Here we demonstrated that GLP-1(9–36) exerts its effects through PI3K/Akt/NOS signaling pathway (Fig. 8).

The PI3K/Akt axis is an essential signaling pathway that promotes cell survival and is responsible for regulation of apoptosis<sup>19</sup>. The role of PI3K and Akt in the prevention of oxidative stress and apoptosis in cardiac cells has been described. Stimulation of Akt activity is capable of suppressing H<sub>2</sub>O<sub>2</sub> induced apoptosis in cardiac myocytes<sup>44</sup>. Treatment with GLP-1 inhibited palmitate-induced apoptosis in cardiomyocytes, in which this protective effect was blocked by PI3K inhibitor<sup>45</sup>. Furthermore, treatment with exendin-4 provokes the activation of Akt activity in H9c2 cells<sup>12</sup>. Consistent with these studies, blockade of either PI3K activity or Akt activity was able to suppress GLP-1(9–36)-induced the synthesis of antioxidant enzymes and antiapoptotic proteins. GLP-1(9–36) effects on the inhibition of caspase-3 activity and apoptosis were also blocked in the presence of PI3K inhibitor or Akt inhibitor. Collectively, PI3K and Akt are necessary for GLP-1(9–36)-mediated antioxidant and antiapoptotic effects in the heart. We also reported here that GLP-1(9–36) induces the phosphorylation and activation of Akt in the PI3K-dependent way in H9c2 cardiomyoblast, emphasizing that PI3K and Akt act as downstream effectors for GLP-1(9–36) signaling. However, how GLP-1(9–36) regulate the activation of PI3K is not known and further study is needed to identify the mechanism for GLP-1(9–36)-mediated PI3K activation in the heart.

Nitric oxide synthase (NOS) is recognized as one of the important effectors of Akt in which Akt mediates phosphorylation and activation of NOS<sup>46,47</sup>. The important role of NOS in protecting the cells has been described and might be reflected on NO production in the cells<sup>48,49</sup>. Our results showed that blockade of NOS inhibited the cardioprotective effects of GLP-1(9–36) against H<sub>2</sub>O<sub>2</sub>, evidenced by a decrease in ROS production and caspase-3 activity. Moreover, depletion of NOS activity also attenuated GLP-1(9–36)-induced the upregulation of antioxidant enzymes (Fig. 6) and antiapoptotic proteins (Fig. 7) in H9c2 cardiomyoblasts.

In HUVECs, GLP-1 induced eNOS synthesis and activity via both the GLP-1R-dependent and GLP-1(9–36)-dependent manners<sup>22</sup>. GLP-1(9–36), but not exendin-4, protected the cells from exposure to I/R or H<sub>2</sub>O<sub>2</sub> via the NOS-dependent way in human aortic endothelial cells isolated from GLP-1R knockout mice<sup>18</sup>. In addition, nNOS-mediated pathway has an essential role in protection of the heart from I/R injury<sup>50</sup>. Consistent with these previous studies, we demonstrated that GLP-1(9–36) increased the synthesis of nNOS and eNOS, leading to an increase in NO levels in H9c2 cardiomyoblasts. In contrast, GLP-1(9–36) had no effect on iNOS mRNA expression. Inhibition of PI3K/Akt pathway using specific PI3K and Akt inhibitors attenuated GLP-1(9–36)-mediated NO production. Thus, cardioprotective effects of GLP-1(9–36) were mainly related to upregulation of nNOS and eNOS through PI3K/Akt axis. Our data support a

concept whereby a cleavage product of GLP-1, GLP-1(9–36) provokes cardioprotective effects in *ex vivo* and *in vivo* models of cardiac injury.

In conclusion, we have revealed novel insights into the molecular mechanisms of a truncated metabolite of GLP-1 hormone, GLP-1(9–36) for cardioprotective effects against oxidative stress and apoptosis (Fig. 8). GLP-1(9–36) exhibits antioxidant effects by reducing ROS production and enhancing the expressions of catalase, GPx-1, and HO-1, and exerts antiapoptotic effects by inhibiting caspase-3 activity and inducing Bcl-2 and Bcl-xL synthesis. These protective effects of GLP-1(9–36) are mediated through PI3K/Akt/NOS signaling pathway.

## Materials And Methods

### Materials

GLP-1(9-36), Exendin-4, exendin fragment 9-39, hydrogen peroxide ( $H_2O_2$ ), and protease inhibitor cocktail were purchased from Sigma-Aldrich (Saint Louis, MO). 2',7'-dichlorodihydrofluorescin diacetate (DCFH-DA), 2 $\beta$ ,5 $\beta$ -Dideoxyadenosine (DDA), LY294002, **PKA inhibitor 14-22 amide (PKI)**, ESI-09, and Akti-1/2 (Akt inhibitor VIII) were obtained from Calbiochem (San Diego, CA). PKC(19-36) (PKC inhibitor) was purchased from Tocris Bioscience (Ellisville, MO). Dulbecco's Modified Eagle Medium (DMEM), fetal bovine serum (FBS), phosphate buffer saline (PBS), penicillin/streptomycin solution, and 0.25% trypsin-EDTA solution were obtained from Gibco (Grand Island, NY).

### Cell culture

H9c2 cardiomyoblasts were obtained from the American Type Culture Collection (ATCC CRL-1446). Cells were grown and cultured in DMEM supplemented with 10% FBS 100 U/mL penicillin, and 100  $\mu$ g/mL streptomycin in a humidified atmosphere of 5 %  $CO_2$  at 37 °C. After approximately reaching 80% - 90 % confluence, cells were detached by trypsinization with 0.25% trypsin-EDTA solution to maintain the logarithmic phase of growth.

### Intracellular ROS measurement

Intracellular ROS level was fluorometrically determined with a fluorogenic dye, DCFH-DA as previously described<sup>10</sup>. Briefly, H9c2 cells were seeded ( $1 \times 10^5$  cells/well) in a 12-well plate and grown overnight. Under serum-free condition, cells were treated with GLP-1(9-36) for 6 h in the presence or absence of specific inhibitors and then incubated with 100  $\mu$ M  $H_2O_2$  for 30 min. Following treatment, medium was replaced with phenol red-free medium and cells were incubated with 10  $\mu$ M DCFH-DA under light protection for 15 min. The DCF fluorescent intensity was detected by a Clariostar fluorometric microplate reader (BMG Labtech) at wavelengths of 485 nm for excitation and 528 nm for emission ( $\lambda_{Ex}/\lambda_{Em} = 485/535$  nm).

### Dihydroethidium (DHE) staining assay

The intracellular ROS level was analyzed using a fluorogenic dye, DHE that is useful for the detection of ROS as previously described<sup>51</sup>. H9c2 cells were seeded in 12-well plate ( $1 \times 10^5$  cells/well) containing gelatin-coated cover slips for overnight. Under serum-free condition, cells were treated with GLP-1(9-36) for 6 h in the presence or absence of specific inhibitors and then incubated with  $H_2O_2$  for 30 min. After treatment, cells were incubated with DHE solution (2  $\mu$ M) for 30 min at 37 °C. After that, cells were fixed with 4% paraformaldehyde in PBS, pH 7.4. After washing, cells were mounted onto microscope slides using Prolong Diamond Antifade Mountant containing DAPI. The fluorescence intensity of DHE labelled cells was visualized with an IX81 fluorescent microscope (Olympus; 20x objective lens). **TUNEL staining assay**

Apoptosis in H9c2 cells was determined by the terminal deoxyribonucleotidyl transferase-mediated triphosphate (dUTP)-biotin nick end labelling (TUNEL) assay<sup>12</sup>. Cells were grown on gelatin-coated glass coverslips in a 12-well plate ( $1 \times 10^5$  cells/well) overnight. Under serum-free condition, cells were treated with GLP-1(9-36) in the presence or absence of specific inhibitors and then incubated with  $H_2O_2$  for 24 h. After treatment, cells were fixed with 4% paraformaldehyde in PBS, pH 7.4, then permeabilized with 0.1% Triton X-100, and subjected to the TUNEL staining using an *in situ* cell death detection kit (Roche Diagnostics). Cells were mounted onto microscope slides using Prolong Diamond Antifade Mountant containing DAPI. Apoptotic cells were determined by counting at least 100 cells in 2-3 randomly selected fields. The percentage of TUNEL positive cells was calculated using the formula ([numbers of TUNEL-positive cells/total number of cells] x 100)

### Caspase-3 activity assay

Caspase-3 activity was evaluated using a caspase-3 colorimetric assay kit (Abcam) as previously described<sup>10</sup> with slight modifications. Briefly, cells were seeded in a 6-well plate ( $2 \times 10^5$  cells/well) overnight. Under serum-free condition, cells were treated with GLP-1(9-36) for 6 h in the presence or absence of specific inhibitors and then incubated with  $H_2O_2$  for 3 h. Following treatment, cells were washed, lysed and centrifuged for 5 min at 12,000 x g at 4 °C. The supernatants were then incubated with caspase-3 substrate (Asp-Glu-Val-Asp p-nitroaniline; DEVD-p-NA) for 1 h at 37 °C. The cleaved substrate p-nitroaniline (p-NA) was determined using a Clariostar microplate reader (BMG Labtech) at 405 nm.

### Western blotting

After treatment, cells were lysed in Triton X-100 lysis buffer containing phenylmethylsulfonyl fluoride and protease inhibitor cocktail as previously described<sup>52</sup>. Protein concentration of cell lysate was determined with a protein assay kit according to the manufacturer's instruction manual (Bio-Rad). Equal amount of protein samples were mixed with an equal volume of 4xSDS loading buffer, denatured and separated by 10% SDS-PAGE gels. Separated proteins were blotted to PVDF membrane, and blocked in 5% non-fat milk. The membranes were incubated with specific antibodies against Akt (Cell Signaling), phosphorylated Akt (Cell Signaling), HO-1 (Cell Signaling), catalase (Cell Signaling), GPx-1 (Abcam) and GAPDH (Santa Cruz). The membranes were incubated with horseradish peroxide-conjugated secondary antibodies (Amersham)

and protein bands were visualized using a Gel Doc™ XR imaging system (Bio-Rad) with a SuperSignal chemiluminescent detection system (Thermo Scientific). The bands were analyzed using ImageJ software.

### Measurement of cAMP level by ELISA

cAMP levels were measured by a cAMP ELISA kit (Cayman) as previously described<sup>53</sup> with slight modifications. Cells were seeded in a 6-well plate ( $2 \times 10^5$  cells/well) overnight. Under serum-free condition, cells were pretreated with IBMX (0.5 mM) for 1 h, and then stimulated with GLP-1(9-36) for 30 min in the presence or absence of specific inhibitors. After treatment, cells were washed and lysed in 0.15% Triton X-100 containing 0.1 M HCl. The intracellular cAMP level was expressed as pmol per mg protein.

### Measurement of nitric oxide (NO) production

The assessment of NO production was performed using nitric oxide assay kit (Abcam) according to the manufacturer's instruction. NO is rapidly oxidized to nitrite and nitrate which are used to measure NO levels. H9c2 cells were seeded in a 6-well plate ( $2 \times 10^5$  cells/well) overnight. Under serum-free condition, cells were pretreated with specific inhibitors for 1 h, and then stimulated with GLP-1(9-36) for 6 h. The calculation of nitrate concentration in the samples was calculated from the standard curve as described in the manufacturer's instruction. The amount of nitrates accurately reflects NO production in the samples.

### mRNA analysis by real time qRT-PCR

The total RNA was extracted from H9c2 cells with RNA isolation kit (Thermo Scientific). The levels of mRNA transcripts were quantified with AriaMx real-time PCR system (Agilent) using SYBR FAST One-step qRT-PCR kits (KAPA Biosystems) according to the manufacturer's protocol. The sequences of primers for rat antioxidative markers (GPx-1, catalase, HO-1, CuZn-SOD, Mn-SOD), pro-apoptotic markers (Bax and Bad) and anti-apoptotic markers (Bcl-2 and Bcl-xL), and nitric oxide synthases (iNOS, eNOS, nNOS) were designed as shown in **Supplementary Table S1**. The expression levels of targeted gene were calculated according to the comparative cycle threshold (CT) method. The fold changes in target gene expression were normalized to GAPDH and determined using  $2^{-\Delta\Delta CT}$ .

### Statistical analysis

Data are expressed as mean  $\pm$  SEM. The statistical analysis was performed with SPSS software (version 18). We used Student's t-test or one-way analysis of variance (ANOVA) with a multiple comparison post hoc test. A p-value less than 0.05 ( $p < 0.05$ ) was considered statistically significant.

### Abbreviations

AC, adenylyl cyclase; Bcl-2, B-cell leukemia-2; Bcl-xL, B-cell lymphoma-extra large; cAMP, cyclic adenosine monophosphate; DAPI, 4',6-diamidino-2-phenylindole; DCFH-DA, Dichlorodihydrofluorescin diacetate; DDA, 2', 5'-dideoxyadenosine; DHE, dihydroethidium; DPP-4, diaminopeptidyl peptidase-4; Epac, exchange protein directly activated by cAMP; GLP-1, glucagon-like peptide-1; GPx-1, glutathione peroxidase-1; HO-1, hemeoxygenase-1; NO, nitric oxide; NOS, nitric oxide synthase; PI3K, phosphoinositide 3-kinase; ROS, reactive oxygen species; SOD, superoxide dismutase; TUNEL, terminal deoxynucleotidyl transferase dUTP nick end labeling

## Declarations

### Acknowledgements

This research was funded by the Thailand Research Fund (TRF) through the Royal Golden Jubilee Ph.D. Program, the Office of the Higher Education Commission, Ministry of Education [Grant PHD/0148/2560] (to N.N. and S.M.) and TRF grant [MRG6180060] (to W.P.). This study is part of a Ph.D. thesis of Biopharmaceutical Sciences Graduate Program, Faculty of Pharmacy, Mahidol University.

### Author contributions

N.N. carried out the experiments, data, and statistical analysis, and wrote the manuscript; W.P. carried out the experiments and data analysis, participated in the study planning, and wrote the manuscript; S.M. performed the experiments, data and statistical analysis, and reviewed/edited the manuscript.

## References

1. Killilea, T. Long-term consequences of type 2 diabetes mellitus: economic impact on society and managed care. *J. Manag. Care.* **8**, S441-449 (2002).
2. Mazzone, T., Chait, A. & Plutzky, J. Cardiovascular disease risk in type 2 diabetes mellitus: insights from mechanistic studies. *Lancet.* **371**, 1800-1809 (2008).
3. Stamler, J., Vaccaro, O., Neaton, J.D. & Wentworth, D. Diabetes, other risk factors, and 12-yr cardiovascular mortality for men screened in the Multiple Risk Factor Intervention Trial. *Diabetes Care.* **16**, 434-444 (1993).
4. Haffner, S.M., Lehto, S., Rönnemaa, T., Pyörälä, K. & Laakso, M. Mortality from coronary heart disease in subjects with type 2 diabetes and in nondiabetic subjects with and without prior myocardial infarction. *Engl. J. Med.* **339**, 229-234 (1998).
5. Pignatelli, P., Menichelli, D., Pastori, D. & Violi, F. Oxidative stress and cardiovascular disease: new insights. *Pol.* **76**, 713-722 (2018).
6. Pastori, D., Carnevale, R. & Pignatelli, P. Is there a clinical role for oxidative stress biomarkers in atherosclerotic diseases? *Intern Emerg Med.* **9**, 123-131 (2014).

7. Murphy, E. & Steenbergen, C. Mechanisms Underlying Acute Protection From Cardiac Ischemia-Reperfusion Injury. *Rev.* **88**, 581-609 (2008).
8. Drucker, D.J. Minireview: the glucagon-like peptides. *142*, 521-527 (2001).
9. Baggio, L.L. & Drucker, D.J. Biology of incretins: GLP-1 and GIP. *132*, 2131-2157 (2007).
10. Mangmool, S., Hemplueksa, P., Parichatikanond, W. & Chattipakorn, N. Epac is required for GLP-1R-mediated inhibition of oxidative stress and apoptosis in cardiomyocytes. *Endocrinol.* **29**, 583-596 (2015).
11. Ban, K. *et al.* Cardioprotective and vasodilatory actions of glucagon-like peptide 1 receptor are mediated through both glucagon-like peptide 1 receptor-dependent and -independent pathways. *Circulation.* **117**, 2340-2350 (2008).
12. Nuamnaichati, N., Mangmool, S., Chattipakorn, N. & Parichatikanond, W. Stimulation of GLP-1 receptor inhibits methylglyoxal-induced mitochondrial dysfunctions in H9c2 cardiomyoblasts: potential role of epac/PI3K/Akt pathway. *Pharmacol.* **11**, 805 (2020).
13. Deacon, C.F. Circulation and degradation of GIP and GLP-1. *Metab. Res.* **36**, 761-765 (2004).
14. Rolin, B., Deacon, C.F., Carr, R.D. & Ahrén, B. The major glucagon-like peptide-1 metabolite, GLP-1-(9-36)-amide, does not affect glucose or insulin levels in mice. *J. Pharmacol.* **494**, 283-288 (2004).
15. Ma, T. *et al.* Glucagon-like peptide-1 cleavage product GLP-1(9-36) amide rescues synaptic plasticity and memory deficits in Alzheimer's disease model mice. *J Neurosci.* **32**, 13701-13708 (2012).
16. Nikolaidis, L.A., Elahi, D., Shen, Y.T. & Shannon, R.P. Active metabolite of GLP-1 mediates myocardial glucose uptake and improves left ventricular performance in conscious dogs with dilated cardiomyopathy. *J. Physiol. Heart Circ. Physiol.* **289**, H2401-2408 (2005).
17. Picatoste, B. *et al.* Sitagliptin reduces cardiac apoptosis, hypertrophy and fibrosis primarily by insulin-independent mechanisms in experimental type-II diabetes. Potential roles of GLP-1 isoforms. *PloS one.* **8**, e78330 (2013).
18. Ban, K. *et al.* Glucagon-like peptide (GLP)-1(9-36)amide-mediated cytoprotection is blocked by exendin(9-39) yet does not require the known GLP-1 receptor. *151*, 1520-1531 (2010).
19. Shaw, R.J. & Cantley, L.C. Ras, PI(3)K and mTOR signalling controls tumour cell growth. *441*, 424-430 (2006).
20. Song, H.P., Chu, Z.G., Zhang, D.X., Dang, Y.M. & Zhang, Q. PI3K-AKT pathway protects cardiomyocytes against hypoxia-induced apoptosis by MitoKATP-Mediated mitochondrial translocation of pAKT. *Physiol. Biochem.* **49**, 717-727 (2018).
21. Mullonkal, C.J. & Toledo-Pereyra, L.H. Akt in ischemia and reperfusion. *Investig. Surg.* **20**, 195-203 (2007).
22. Ding, L. & Zhang, J. Glucagon-like peptide-1 activates endothelial nitric oxide synthase in human umbilical vein endothelial cells. *Acta Pharmacol. Sin.* **33**, 75-81 (2012).
23. Bae, S. *et al.* Hydrogen peroxide-responsive nanoparticle reduces myocardial ischemia/reperfusion injury. *Am. Heart Assoc.* **5**, (2016).

24. Xiang, J., Wan, C., Guo, R. & Guo, D. Is Hydrogen peroxide a suitable apoptosis inducer for all cell types? *BioMed Res. Int.* **2016**, 7343965 (2016).
25. Green, B.D. *et al.* GLP-1 and related peptides cause concentration-dependent relaxation of rat aorta through a pathway involving KATP and cAMP. *Biochem. Biophys.* **478**, 136-142 (2008).
26. Koundouros, N. & Poulogiannis, G. Phosphoinositide 3-Kinase/Akt Signaling and Redox Metabolism in Cancer. *Oncol.* **8**, 160 (2018).
27. Kim, H. & Kang, P.M. Apoptosis in cardiovascular diseases: mechanism and clinical implications. *Korean Circ. J.* **40**, 299-305 (2010).
28. Teringova, E. & Tousek, P. Apoptosis in ischemic heart disease. *Transl. Med.* **15**, 87 (2017).
29. Narula, J. *et al.* Apoptosis in myocytes in end-stage heart failure. *Engl. J. Med.* **335**, 1182-1189 (1996).
30. Olivetti, G. *et al.* Acute myocardial infarction in humans is associated with activation of programmed myocyte cell death in the surviving portion of the heart. *Mol. Cell. Cardiol.* **28**, 2005-2016 (1996).
31. Chou, H.C. & Chan, H.L. 5-Methoxytryptophan-dependent protection of cardiomyocytes from heart ischemia reperfusion injury. *Biochem. Biophys.* **543**, 15-22 (2014).
32. Yoon, J.S. & Lee, H.W. Understanding the cardiovascular effects of incretin. *Diabetes Obes. Metab.* **35**, 437-443 (2011).
33. Giacco, F. *et al.* GLP-1 cleavage product reverses persistent ROS generation after transient hyperglycemia by disrupting an ROS-Generating feedback loop. *64*, 3273-3284 (2015).
34. Göke, R. *et al.* Exendin-4 is a high potency agonist and truncated exendin-(9–39)-amide an antagonist at the glucagon-like peptide 1-(7-36)-amide receptor of insulin-secreting beta-cells. *Biol. Chem.* **268**, 19650–5 (1993)
35. Li, J. *et al.* Cardiovascular benefits of native GLP-1 and its metabolites: an indicator for GLP-1-therapy strategies. *Physiol.* **8**, 15 (2017).
36. Siraj, M.A. *et al.* Cardioprotective GLP-1 metabolite prevents ischemic cardiac injury by inhibiting mitochondrial trifunctional protein-a. *Clin. Investig.* **130**, 1392-1404 (2020)
37. Lamendola, P. *et al.* Mechanisms of myocardial cell protection from ischemia/reperfusion injury and potential clinical implication. *G Ital Cardiol (Rome)*. **10**, 28-36 (2009).
38. Oeseburg, H. *et al.* Glucagon-like peptide 1 prevents reactive oxygen species-induced endothelial cell senescence through the activation of protein kinase A. *Thromb. Vasc. Biol.* **30**, 1407-1414 (2010).
39. Gezginci-Oktayoglu, S., Sacan, O., Yanardag, R., Karatug, A. & Bolkent, S. Exendin-4 improves hepatocyte injury by decreasing proliferation through blocking NGF/TrkA in diabetic mice. *32*, 223-231 (2011).
40. Gross, A., McDonnell, J.M. & Korsmeyer, S.J. BCL-2 family members and the mitochondria in apoptosis. *Genes Dev.* **13**, 1899-1911 (1999).
41. Kale, J., Osterlund, E.J. & Andrews, D.W. BCL-2 family proteins: changing partners in the dance towards death. *Cell Death Differ.* **25**, 65-80 (2018).

42. Porter, A.G. & Jänicke, R.U. Emerging roles of caspase-3 in apoptosis. *Cell Death Differ.* **6**, 99-104 (1999).
43. Noyan-Ashraf, M.H. *et al.* GLP-1R agonist liraglutide activates cytoprotective pathways and improves outcomes after experimental myocardial infarction in mice. **58**, 975-983 (2009).
44. Matsui, T. & Rosenzweig, A. Convergent signal transduction pathways controlling cardiomyocyte survival and function: the role of PI 3-kinase and Akt. *Mol. Cell. Cardiol.* **38**, 63-71 (2005).
45. Ravassa, S., Zudaire, A., Carr, R.D. & Díez, J. Antiapoptotic effects of GLP-1 in murine HL-1 cardiomyocytes. *Am. J. Physiol.* **300**, H1361-1372 (2011).
46. Guerra, D.D. *et al.* Akt phosphorylation of neuronal nitric oxide synthase regulates gastrointestinal motility in mouse ileum. *Natl. Acad. Sci. U.S.A.* **116**, 17541 (2019).
47. Dimmeler, S. *et al.* Activation of nitric oxide synthase in endothelial cells by Akt-dependent phosphorylation. **399**, 601-605 (1999).
48. Wink, D.A. *et al.* Nitric oxide protects against cellular damage and cytotoxicity from reactive oxygen species. *Natl. Acad. Sci. U.S.A.* **90**, 9813-9817 (1993).
49. Li, J., Billiar, T.R., Talanian, R.V. & Kim, Y.M. Nitric oxide reversibly inhibits seven members of the caspase family via S-nitrosylation. *Biophys. Res. Commun.* **240**, 419-424 (1997).
50. Hu, L. *et al.* Ischemic postconditioning protects the heart against ischemia-reperfusion injury via neuronal nitric oxide synthase in the sarcoplasmic reticulum and mitochondria. *Cell Death Dis.* **7**, e2222 (2016).
51. Sudi, S.B. *et al.* TRPC3-Nox2 axis mediates nutritional deficiency-induced cardiomyocyte atrophy. *Rep.* **9**, 9785 (2019).
52. Parichatikanond, W., Nishimura, A., Nishida, M. & Mangmool, S. Prolonged stimulation of  $\beta$ 2-adrenergic receptor with  $\beta$ 2-agonists impairs insulin actions in H9c2 cells. *Pharmacol. Sci.* **138**, 184-191 (2018).
53. Phosri, S., Bunrukchai, K., Parichatikanond, W., Sato, V.H. & Mangmool, S. **Epac is required for exogenous and endogenous stimulation of adenosine A<sub>2B</sub> receptor for inhibition of angiotensin II-induced collagen synthesis and myofibroblast differentiation.** *Purinergic Signal.* **14**, 141-56 (2018).

## Figures

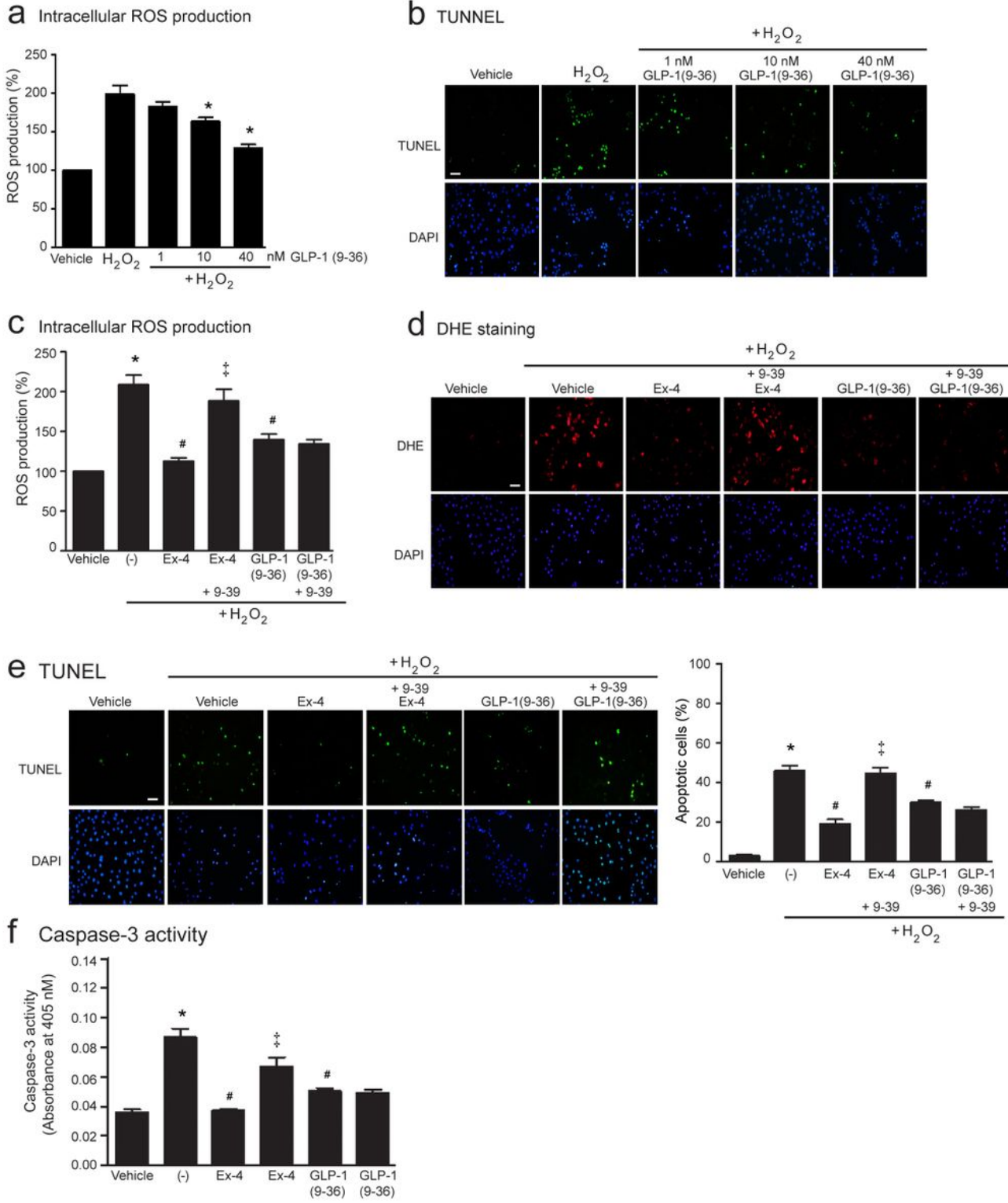


**Figure 1**

GLP-1(9-36) inhibits  $\text{H}_2\text{O}_2$ -induced oxidative stress and apoptosis through GLP-1R-independent way (A,B) H9c2 cells were treated with either vehicle (control) or different doses of GLP-1(9-36) for 6 hours prior to the stimulation with  $\text{H}_2\text{O}_2$  ( $200 \mu\text{M}$ ) for 1 h (A) or 24 h (B). (C-F) Cells were pretreated without or with 100 nM exendin-(9-39) (9-39) for 1 h before treatment with vehicle (control), 20 nM exendin-4 (Ex-4), or 40 nM GLP-1(9-36) for 6 h. Cells were then treated with  $\text{H}_2\text{O}_2$  for 1 h (C, D), 3 h (F), or 24 h (E). (A, C)

Quantification of intracellular ROS was performed by using DCFH-DA and calculated as the percentages relative to the vehicle-treated group. (B,E) Apoptotic cells were detected by TUNEL staining (green). Scale bar, 10  $\mu$ m. The number of apoptotic cells was expressed as the percentage of apoptotic cells over vehicle. (D) The fluorescence intensity of DHE labeled cells (red). Scale bar, 10  $\mu$ m. (F) Caspase-3 activity was evaluated with colorimetric enzymatic assay and calculated from the absorbance values at 405 nm. Data are presented as mean  $\pm$  SEM ( $n = 4$ ). \* $p < 0.05$  vs. vehicle; # $p < 0.05$  vs. H<sub>2</sub>O<sub>2</sub>; ‡ $p < 0.05$  vs. H<sub>2</sub>O<sub>2</sub>+Ex-4.

**Figure 2**

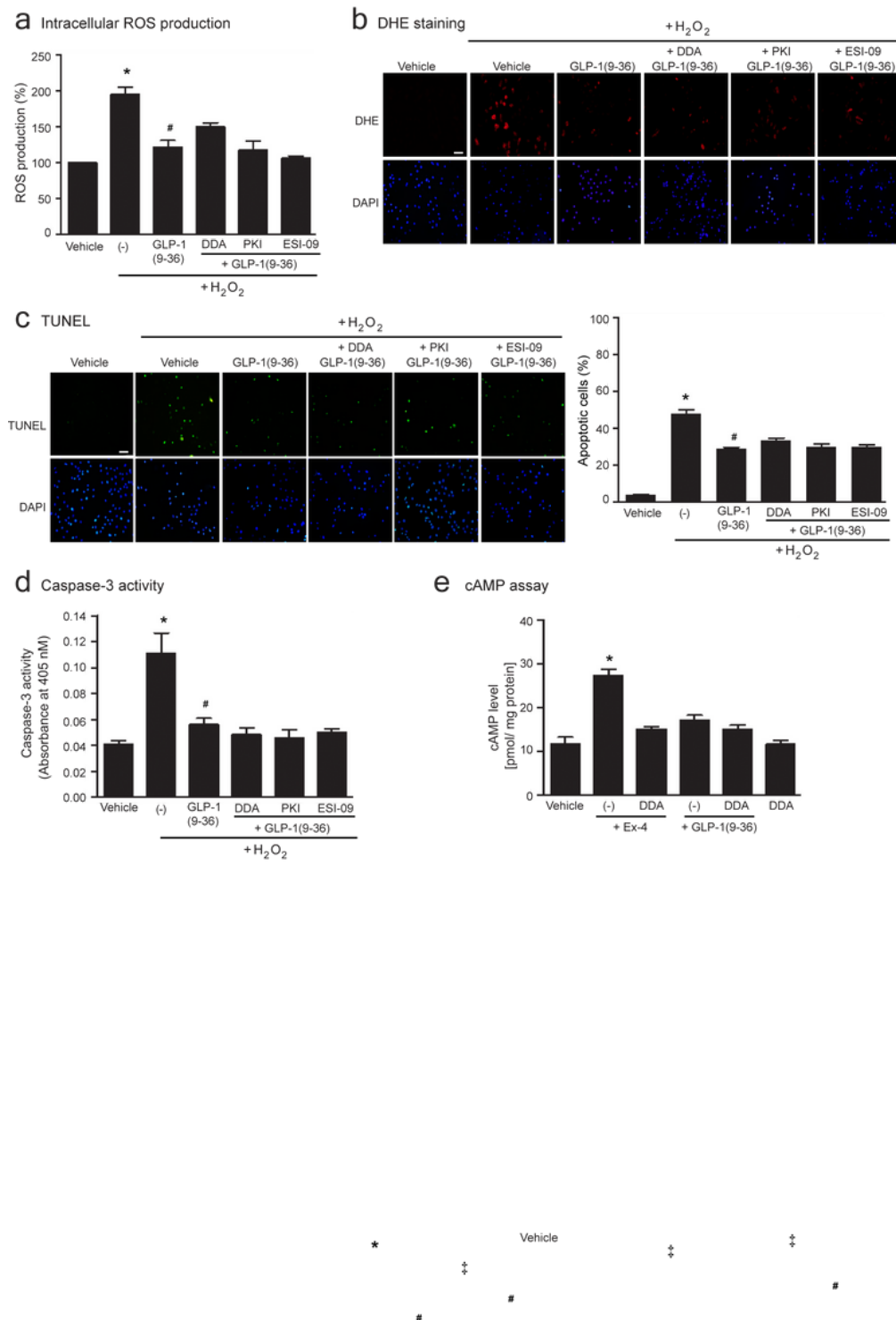


## Figure 2

Antioxidant and antiapoptotic effects of GLP-1(9-36) are independent of cAMP (A-D). Cells were pretreated without or with dideoxyadenosine (DDA; AC inhibitor), PKI (PKA inhibitor), or ESI-09 (Epac inhibitor) for 1 h before treatment with vehicle (control) or 40 nM GLP-1(9-36) for 6 h. Cells were then treated with 200  $\mu$ M H<sub>2</sub>O<sub>2</sub> for 1 h (A, B), 3 h (D), or 24 h (C). (A) Quantification of intracellular ROS was performed by using DCFH-DA and calculated as the percentages relative to the vehicle-treated group. (B) The fluorescence intensity of DHE labeled cells (red). Scale bar, 10  $\mu$ m. (C) Apoptotic cells were detected by TUNEL staining (green). Scale bar, 10  $\mu$ m. The number of apoptotic cells was expressed as the percentage of apoptotic cells over vehicle. (D) Caspase-3 activity was evaluated with colorimetric enzymatic assay and calculated from the absorbance values at 405 nm. (E) Cells were pretreated without or with DDA for 1 h before treatment with 20 nM exendin-4 (Ex-4), or 40 nM GLP-1(9-36) for 30 min. The cAMP levels were calculated and shown as [pmoL/ mg protein]. Data are presented as mean  $\pm$  SEM (n = 4). \*p < 0.05 vs. vehicle; #p < 0.05 vs. Ex-4.

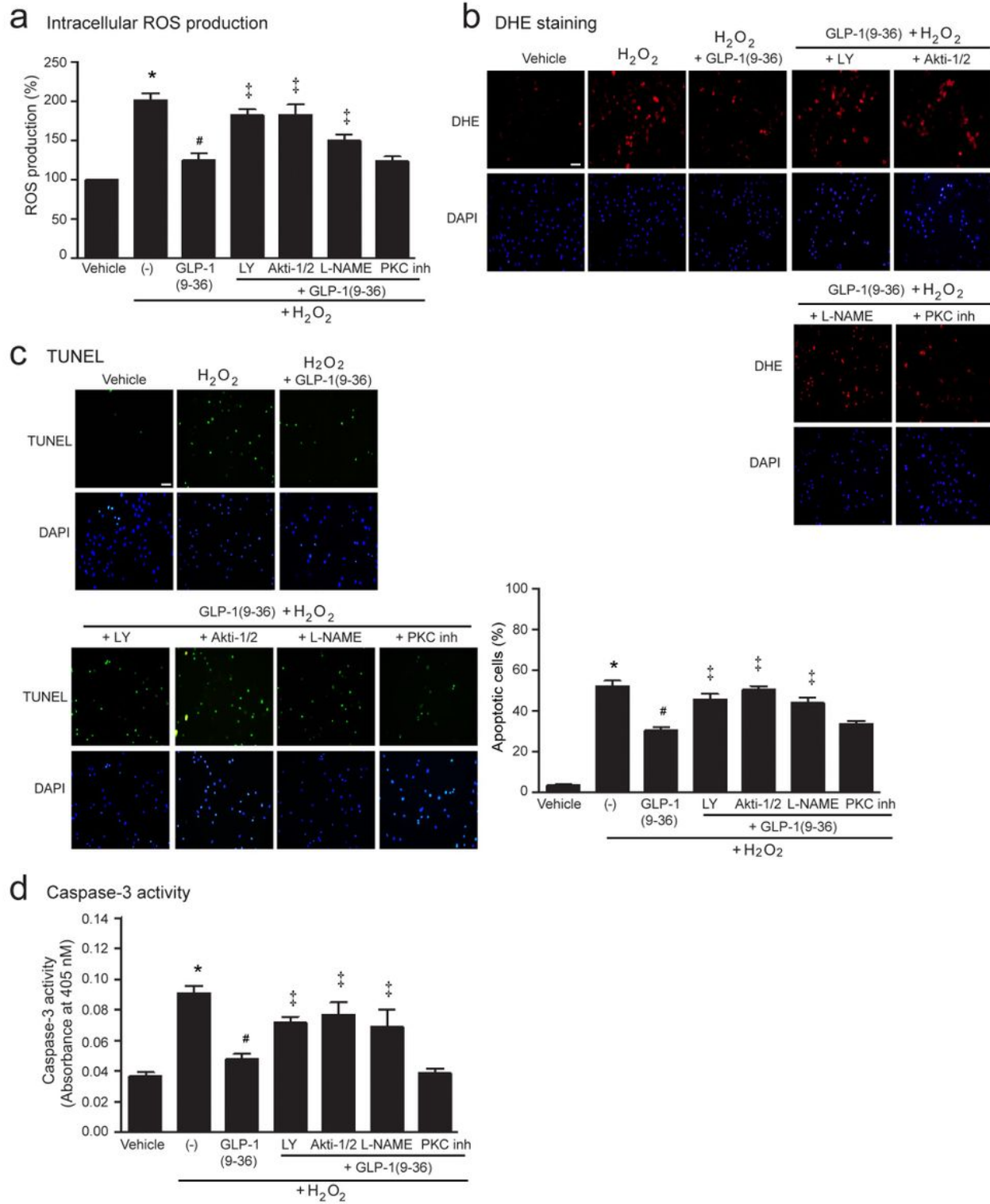


**Figure 3**

Cardioprotective effects of GLP-1(9-36) are mediated through PI3K/Akt/NOS pathway (A-D). Cells were pretreated without or with LY294002 (LY; PI3K inhibitor), Akti-1/2 (Akti-1/2; Akti inhibitor), L-NAME (NOS inhibitor), or PKC inhibitor (PKC inh) for 1 h before treatment with vehicle (control) or 40 nM GLP-1(9-36) for 6 h. Cells were then treated with H<sub>2</sub>O<sub>2</sub> for 1 h (A, B), 3 h (D), or 24 h (C). (A) Quantification of intracellular ROS was performed by using DCFH-DA and calculated as the percentages relative to the

vehicle-treated group. (B) The fluorescence intensity of DHE labeled cells (red). Scale bar, 10  $\mu$ m. (C) Apoptotic cells were detected by TUNEL staining (green). Scale bar, 10  $\mu$ m. The number of apoptotic cells was expressed as the percentage of apoptotic cells over vehicle. (D) Caspase-3 activity was evaluated with colorimetric enzymatic assay and calculated from the absorbance values at 405 nm. Data are presented as mean  $\pm$  SEM ( $n = 4$ ). \* $p < 0.05$  vs. vehicle; # $p < 0.05$  vs. H2O2; ‡ $p < 0.05$  vs. H2O2+GLP-1(9-36).

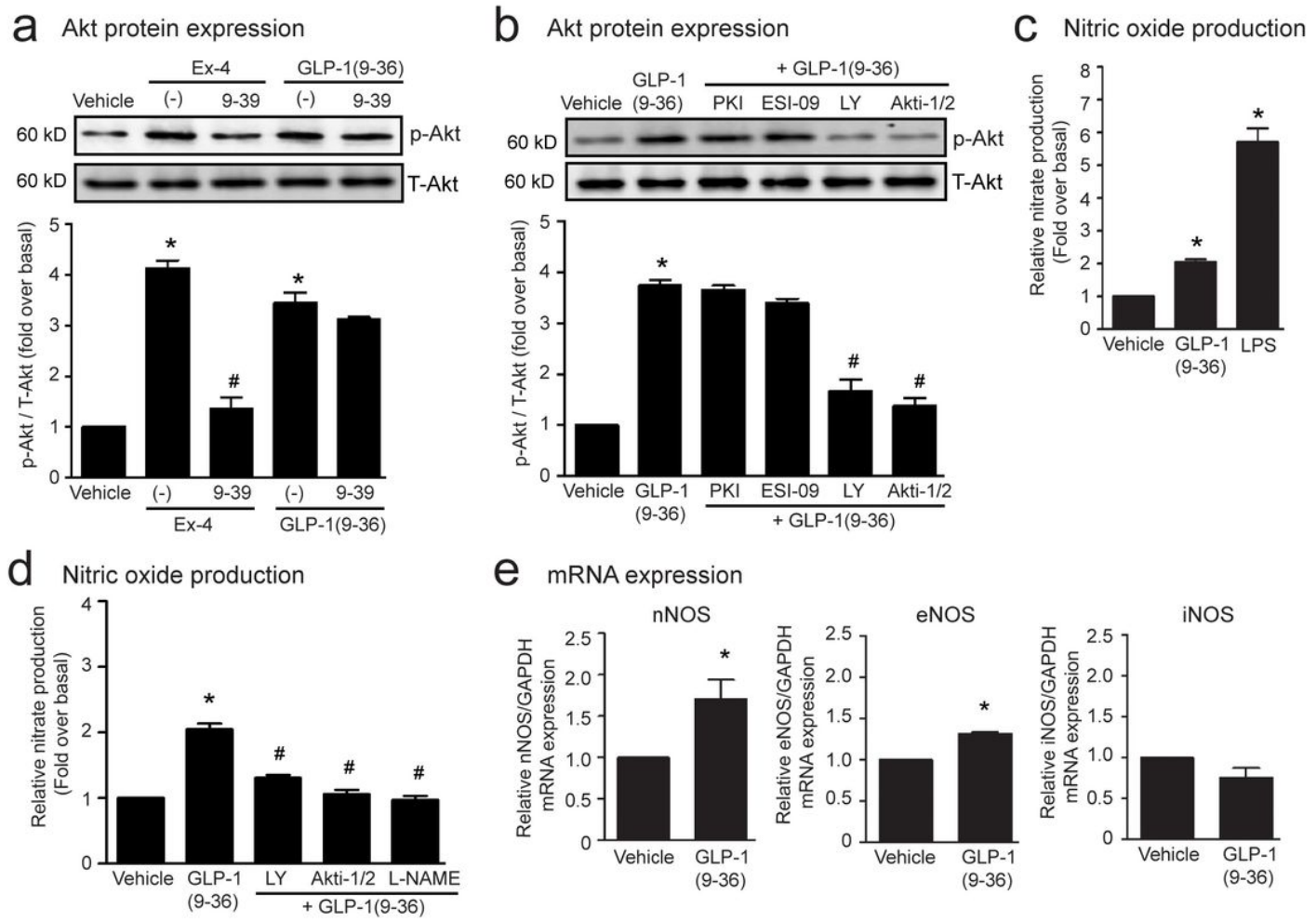
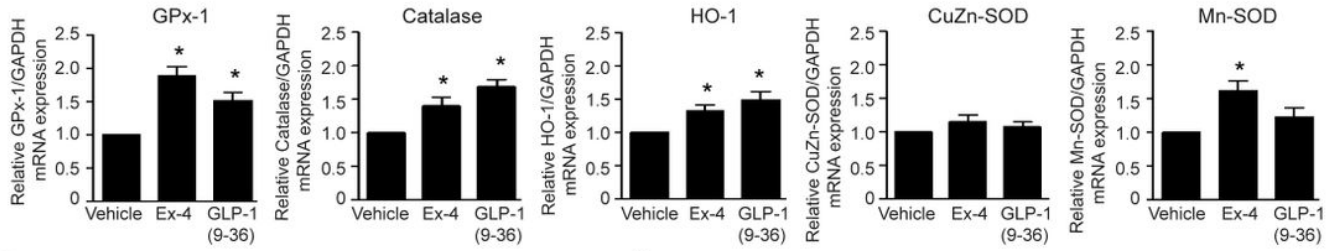


**Figure 4**

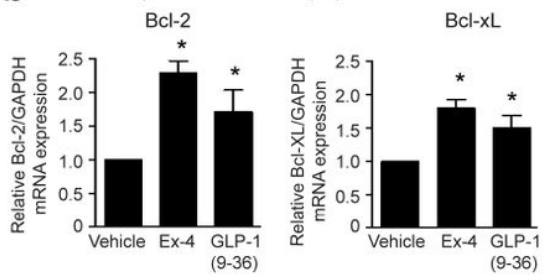
GLP-1(9-36) mediates PI3K-induced Akt phosphorylation and NO production (A) H9c2 cells were pretreated without or with 100 nM exendin-(9-39) (9-39) before treatment with vehicle (control), 20 nM exendin-4 (Ex-4) or 40 nM GLP-1(9-36) for 30 min. (B) Cells were pretreated without or with 100 nM exendin-(9-39) (9-39), 10  $\mu$ M PKI (PKA inhibitor), 10  $\mu$ M ESI-09 (Epac inhibitor), 10  $\mu$ M LY294002 (LY; PI3K inhibitor) or 1  $\mu$ M Akti-1/2 (Akt inh; Akt inhibitor) for 1 h before treatment with vehicle or GLP-1(9-36) for 30 min. (A,B) Akt activation (phospho-Akt/total-Akt) was expressed as fold change over non-stimulated (vehicle-treated) group. (C) Cells were treated with vehicle, GLP-1(9-36), exendin-4 (Ex-4), or 1  $\mu$ g/mL lipopolysaccharide (LPS) for 1 h. (D) Cells were pretreated without or with LY294002, Akti-1/2 or L-NAME for 1 h before treatment with vehicle or GLP-1(9-36) for 1 h. (C,D) Nitric oxide (NO) levels secreted into the

medium were measured using ELISA assay and expressed as fold increase over non-stimulated (vehicle-treated) group. (E) Cells were treated with vehicle or GLP-1(9-36) for 6 h. The mRNA levels of nNOS, eNOS, and iNOS were detected by real time qRT-PCR, normalized with GAPDH, and expressed as fold change over vehicle. Data are presented as mean  $\pm$  SEM ( $n = 4$ ). \* $p < 0.05$  vs. vehicle; # $p < 0.05$  vs. GLP-1 (9-36).

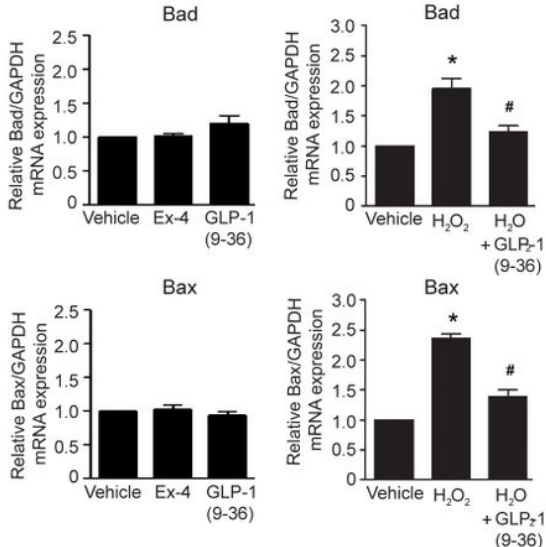
### A mRNA expression of antioxidant markers



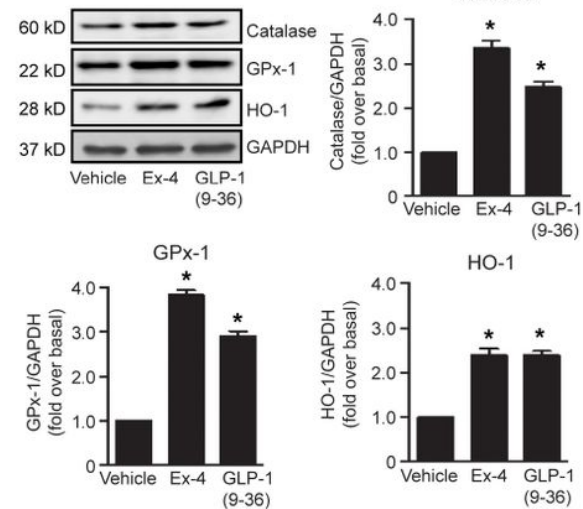
### B mRNA expression of antiapoptotic markers



### C mRNA expression of proapoptotic markers



### D protein expression of antioxidant markers



### E protein expression of antiapoptotic markers

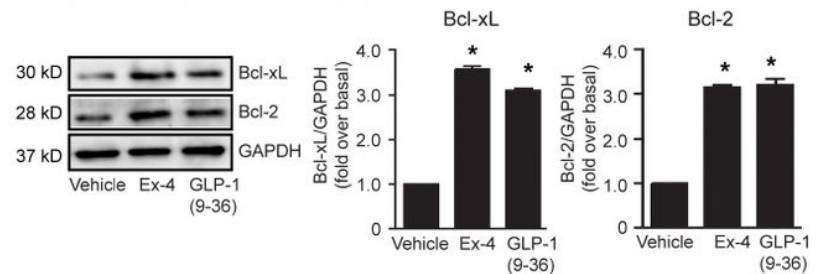
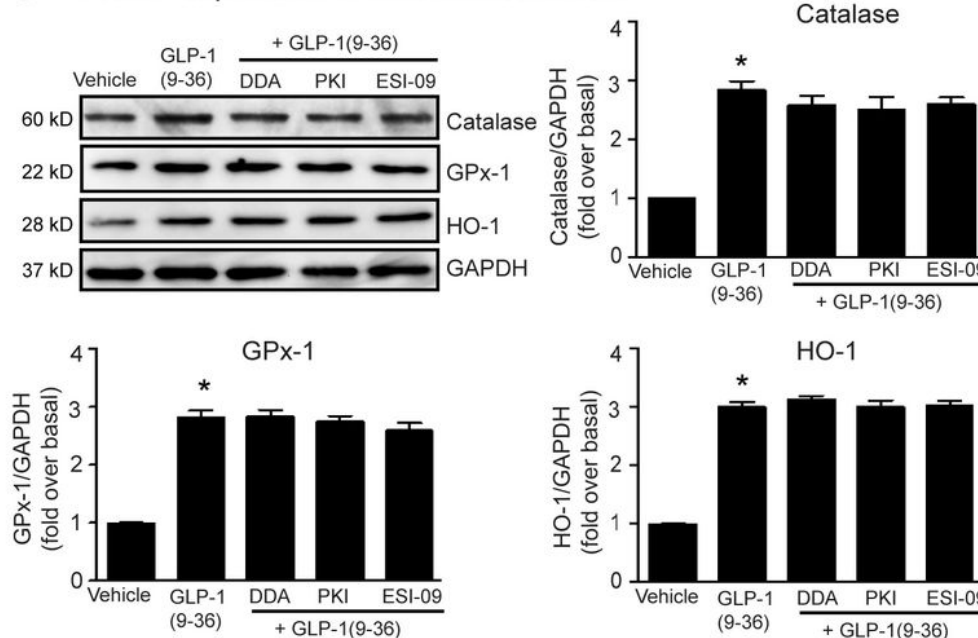


**Figure 5**

Effects of GLP-1 (9-36) on upregulation of antioxidant enzymes and antiapoptotic proteins (A,B) H9c2 cells were treated with vehicle, exendin-4 (Ex-4) or GLP-1(9-36) for 6 h. The mRNA levels of targeted genes were detected by real time qRT-PCR, normalized with GAPDH, and expressed as fold change over vehicle. Data are presented as mean  $\pm$  SEM ( $n = 4$ ). \* $p < 0.05$  vs. vehicle. (C) (left panel) Cells were treated with vehicle, exendin-4 (Ex-4) or GLP-1(9-36) for 6 h. (right panel) Cells were pretreated without or with GLP-1(9-36) before exposure to vehicle (control) or 200  $\mu$ M H<sub>2</sub>O<sub>2</sub> for 6 h. The mRNA levels of targeted genes

were detected by real time qRT-PCR, normalized with GAPDH, and expressed as fold change over vehicle. Data are presented as mean  $\pm$  SEM ( $n = 4$ ). \* $p < 0.05$  vs. vehicle; # $p < 0.05$  vs. H2O2. (D,E) Cells were treated with vehicle, exendin-4 (Ex-4) or GLP-1(9-36) for 24 h. Representative immunoblots were detected by western blotting. The relative protein levels were evaluated and expressed as fold increase over vehicle (basal). Data are presented as mean  $\pm$  SEM ( $n = 4$ ). \* $p < 0.05$  vs. vehicle.

### a Protein expression of antioxidant markers



### b Protein expression of antioxidant markers

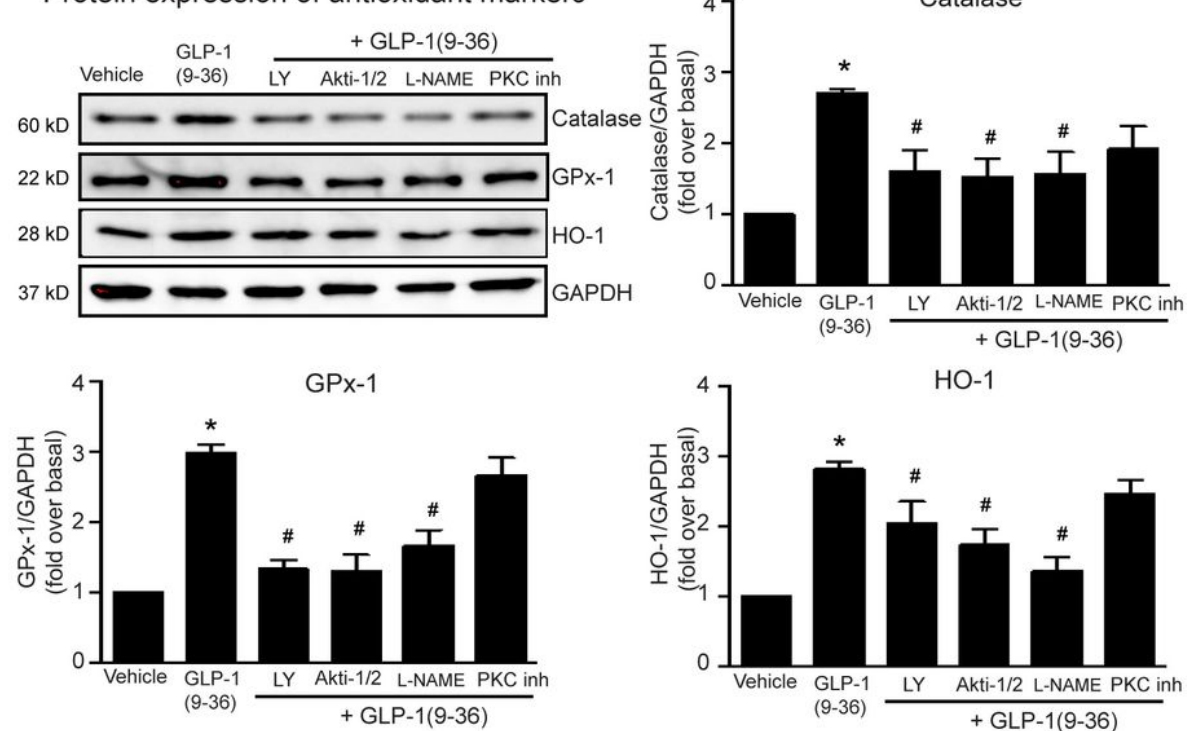
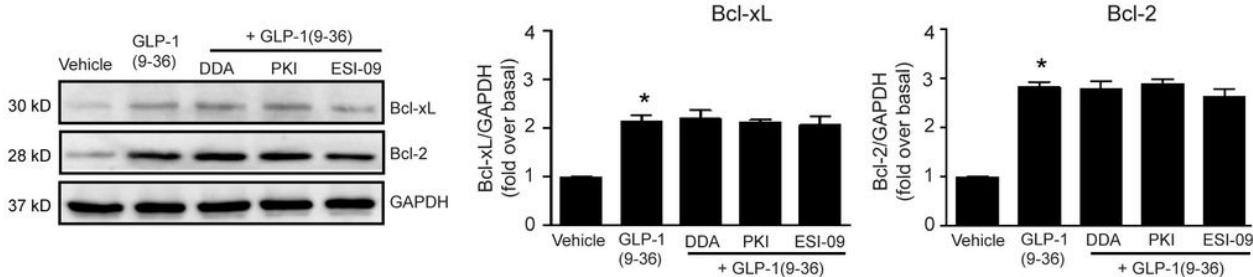


**Figure 6**

GLP-1 (9-36) induces antioxidant enzyme synthesis through a cAMP-independent and PI3K/Akt/NOS-dependent manner (A) H9c2 cells were pretreated without or with DDA (AC inhibitor), PKI (PKA inhibitor), or ESI-09 (Epac inhibitor) for 1 h before treatment with vehicle (control) or 40 nM GLP-1(9-36) for 24 h. (B) Cells were pretreated without or with LY294002 (LY; PI3K inhibitor), Akti-1/2 (Akt inh; Akt inhibitor), L-NAME (NOS inhibitor) or PKC inh (PKC inhibitor) for 1 h before treatment with vehicle or GLP-1(9-36) for 24 h. (A,B) Representative immunoblots were detected by western blotting. The relative protein levels were evaluated and expressed as fold increase over vehicle (basal). Data are presented as mean  $\pm$  SEM ( $n = 4$ ). \* $p < 0.05$  vs. vehicle; # $p < 0.05$  vs. GLP-1 (9-36).

**a Protein expression of antiapoptotic markers**



**b Protein expression of antiapoptotic markers**

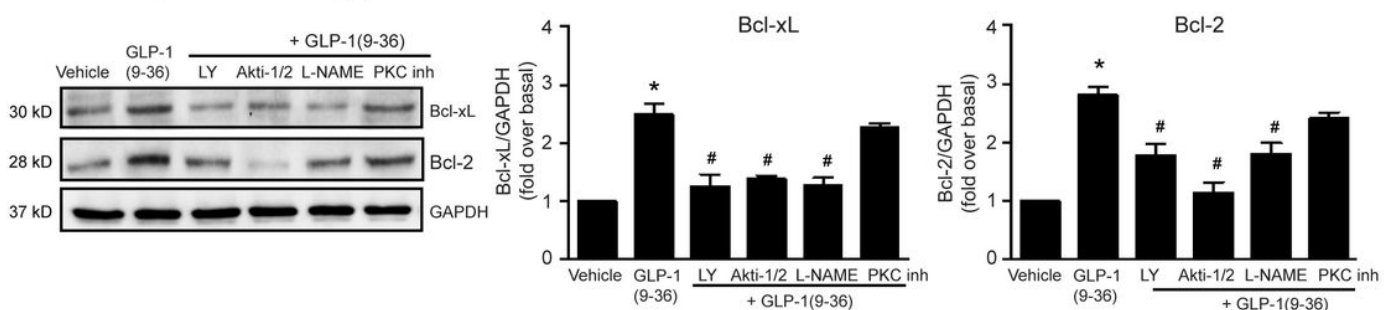
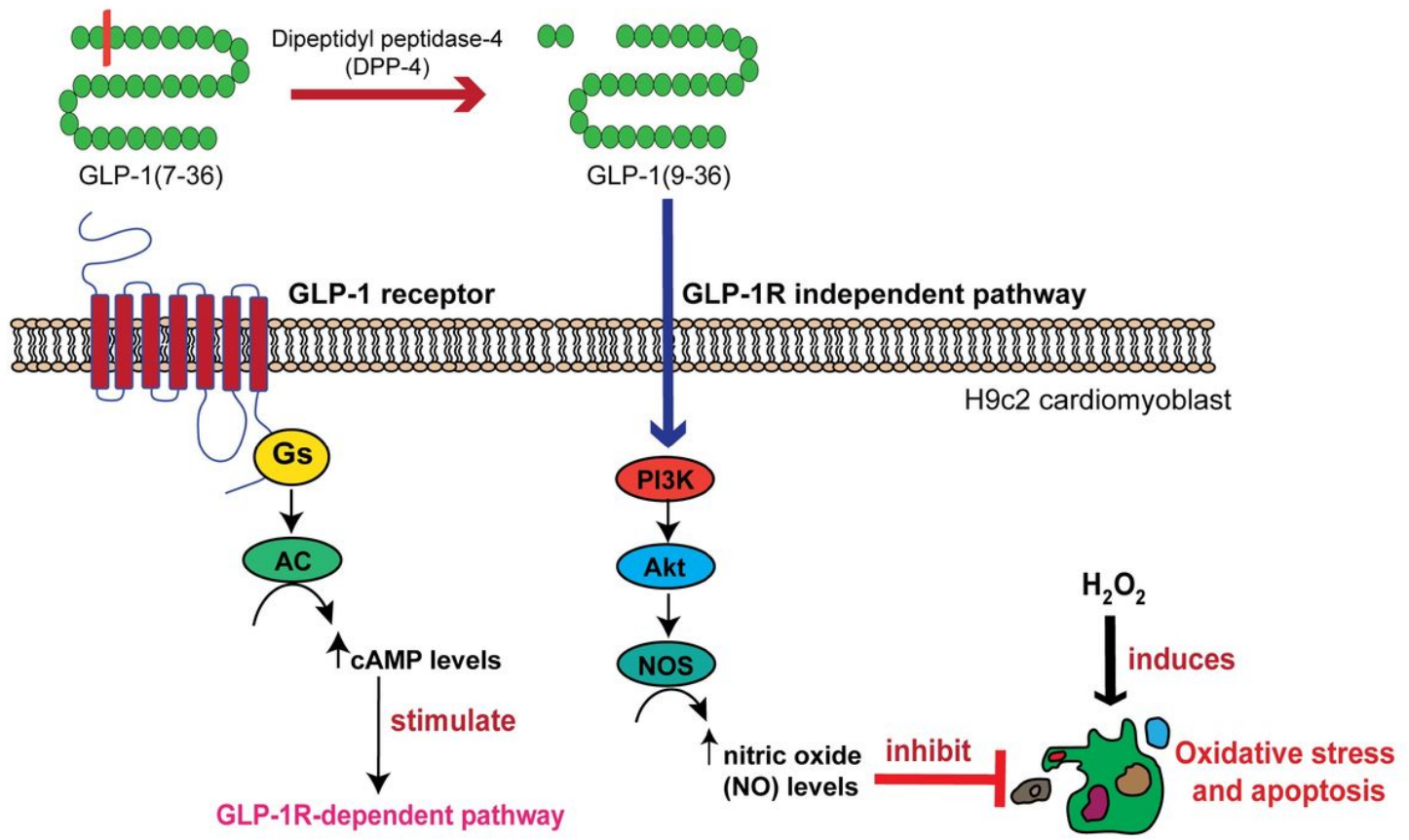


**Figure 7**

GLP-1 (9-36) mediates antiapoptotic protein synthesis through a cAMP-independent and PI3K/Akt/NOS-dependent manner (A) H9c2 cells were pretreated without or with DDA (AC inhibitor), PKI (PKA inhibitor), or ESI-09 (Epac inhibitor) for 1 h before treatment with vehicle (control) or 40 nM GLP-1(9-36) for 24 h. (B) Cells were pretreated without or with LY294002 (LY; PI3K inhibitor), Akti-1/2 (Akt inh; Akt inhibitor), L-NAME (NOS inhibitor) or PKC inh (PKC inhibitor) for 1 h before treatment with vehicle or GLP-1(9-36) for 24 h. (A,B) Representative immunoblots were detected by western blotting. The relative protein levels were evaluated and expressed as fold increase over vehicle (basal). Data are presented as mean  $\pm$  SEM ( $n = 4$ ). \* $p < 0.05$  vs. vehicle; # $p < 0.05$  vs. GLP-1 (9-36).



#### Cardioprotective effects of GLP-1(9-36)

- Antioxidant effects by ↑ catalase, GPx-1 & HO-1 synthesis
- Antiapoptotic effects by ↑ Bcl-2 & Bcl-xL synthesis, and ↓ caspase-3 activity

**Figure 8**

Schematic representing the mechanism by which GLP-1(9-36) protects against oxidative stress and apoptosis via activating the PI3K/Akt/NOS pathway. GLP-1(7-36) binds to and stimulates GLP-1R which exerts protective effects through GLP-1R-dependent way. GLP-1(7-36) is cleaved by dipeptidyl peptidase-4 (DPP-4) to generate a truncated metabolite, GLP-1(9-36) which has a low affinity for GLP-1 receptor (GLP-1R). In cardiomyoblasts, GLP-1(9-36) possesses antioxidant effects by increasing the synthesis of catalase, GPx-1 and HO-1, and elicits antiapoptotic effects by increasing the synthesis of Bcl-2 and Bcl-xL, and reducing caspase-3 activity. These cardioprotective effects of GLP-1(9-36) are mediated through PI3K/Akt/NOS signaling pathway.

## Supplementary Files

This is a list of supplementary files associated with this preprint. Click to download.

- GLP1936supplementaryinformation.doc